



ON SOUND PROPAGATION IN A LINEAR SHEAR FLOW

L. M. B. C. CAMPOS, J. M. G. S. OLIVEIRA AND M. H. KOBAYASHI

*Secção de Mecânica Aeroespacial, ISR, Instituto Superior Técnico,
1096 Lisboa Codex, Portugal*

(Received 24 March 1997, and in final form 14 May 1998)

It is shown that the acoustic wave equation in a linear shear flow always has a critical layer, where the Doppler shifted frequency vanishes; since this is the only singularity of the wave equation apart from the point at infinity, the power series solution about the critical layer has infinite radius of convergence. Two linearly independent solutions are even and odd functions of distance from the critical layer. Their plots show that acoustic oscillations are suppressed near the critical layer. A linear combination of these solutions specifies the general acoustic field; the constants of integration are determined from boundary conditions of which several examples are given. The total acoustic field is illustrated for rigid and impedance wall conditions. The cases illustrated include both real and complex wave fields. These wave fields are small amplitude perturbations of the acoustic wave equation in a linear shear flow; it is shown (in the Appendix) that the perturbations of vorticity and dilatation are coupled, and thus combine features of “acoustic” and “hydrodynamic” modes.

© 1999 Academic Press

1. INTRODUCTION

The wave equation describing the propagation of sound in a transversely sheared unidirectional flow [1, 2], has been solved mostly by approximate methods, either analytical or numerical [3–18]. Exact analytical solutions appear in the literature only in one case, concerning sound propagation in a linear shear flow in three forms: (i) in terms of parabolic cylinder functions [19], for an unbounded linear velocity profile; (ii) in terms of Whittaker functions [20, 21] for a linear velocity profile or a linear velocity matching two uniform streams, to represent a shear layer; (iii) in terms of confluent hypergeometric functions, for a linear velocity profile, or a linear velocity matched to a uniform stream to represent a boundary layer [22–24]. Series solutions without explicit reference to a particular special functions had been obtained before [25, 26]. In the present paper the linear velocity profile is reconsidered, to show that in this case the acoustic wave equation has a regular singularity, which has been used as expansion point in the analysis appearing in the literature. This singularity corresponds to the vanishing of the Doppler shifted frequency, and thus may occur for other velocity profiles as well. This is an instance of the occurrence in acoustics of the critical layer which has

been studied extensively for other types of waves: e.g., internal [27–29], inertial [30], instability [31], acoustic–gravity [32–34] and hydromagnetic [35–41].

In contrast to the acoustics of quasi-one-dimensional “plug” flow in a nozzle of varying cross-section [42–44] for which several exact solutions exist [45–51], the only exact solution for a sheared mean flow is for the case of a linear velocity profile which, through different changes of variable, has been expressed in terms of parabolic cylinder functions [19], Whittaker functions [20, 21] or confluent hypergeometric functions [22–24]. There has been perhaps insufficient attention to the physical effects underlying these mathematical solutions: viz., the existence of a critical layer, where sound can be absorbed or reflected. The critical layer for sound in a shear flow corresponds to the “turning point” identified in connection with some approximate methods [13, 14, 52]; the ray theory [53–55] does not apply at such a singularity, where the usual forms of conservation of wave action break down [56, 57]. Some of the literature leaves unmentioned the existence of a critical layer [19], whereas in other cases its relevance is perhaps too lightly dismissed as a feature worthy of less attention [12]. In fact, a critical layer is always present in the acoustics of a linear shear flow, and it plays a central role in the solution of the wave equation, because it is the only singularity at finite distance; thus (i) a series expansion about any point y_1 other than the critical layer y_c , would have its radius of convergence limited by $|y - y_1| \leq R \equiv |y_c - y_1|$ by it, and (ii) a series expansion about the critical layer has an infinite radius of convergence: i.e., it covers the whole flow region. The latter solution (ii) can be obtained by the classical Frobenius–Fuchs method [58–62], and is suitable for a discussion of the physics of the interaction of sound with flow.

After a discussion of the literature in the introduction, the starting point for the present work is the presentation of the method of solution of the acoustic wave equation (Figure 1) in a linear shear flow (section 2). Upon taking as an example an earlier solution [19], it is shown that the critical layer was implicitly used as the center for a power series expansion (section 2.1). Making an explicit change of independent variable, which places the critical layer at the origin, and the wall (or point of zero flow velocity) at position unity (section 2.2), leads, without any further transformations, to a second order differential equation with variable coefficients, which has the critical layer as a regular singularity and the point at infinity as an irregular singularity (section 2.3). Although the latter irregular singularity is of higher degree than those for the parabolic cylinder or confluent hypergeometric function, an exact solution can (section 3) still be obtained by the Frobenius–Fuchs method (section 3.1); this solution involves a linear combination of even and odd functions of the distance from the critical layer (section 3.2) which are plotted (Figures 2–5) for several values of the two dimensionless parameters of the problem giving (section 3.3) real waveforms. By a further change of independent variable, which places the wall at a variable (not necessarily unit) distance from the critical layer, the problem is reduced to a single parameter (section 4) thus simplifying the plotting of solutions (Figures 6, 7 and 8); the latter parameter is complex in the case (Figures 13 to 15) of complex wavenumber (section 4.1). Complex solutions also occur for certain types of boundary conditions, e.g., an impedance wall (section 4.2) leads to a complex wavefield

(Figures 9, 11, 12, 16 and 17), whereas a rigid wall leads to a real waveform (Figure 10), if the other boundary condition is real (section 4.3). The discussion addresses the issue of the distinction [2, 12] between “acoustic” and “hydrodynamic” modes, and the appendix shows that for sound in a linear shear flow the vorticity and dilatation are coupled. The present discussion shows that the role of the critical layer in acoustics [63, 64] is not dissimilar to that in other branches of wave theory [65, 66].

2. METHOD OF EXACT SOLUTION

The examination of one of the solutions in the literature [19] shows that the critical layer has implicitly been taken as center for a power series expansion; the latter can be obtained quite simply, when using the standard Frobenius–Fuchs method, via a simple change of independent variable which places the critical layer at the origin and the wall at position unity; no changes of dependent variable are needed, and the series solutions follow without need to refer to particular special functions.

2.1. EXAMINATION OF A PREVIOUS SOLUTION

The acoustic pressure p in a steady mean homentropic flow, in the x direction, sheared in the y direction, satisfies the wave equation [2]

$$(d/dt)((1/c^2)d^2p/dt^2 - \nabla^2 p) - 2(dU/dy)\partial^2 p/\partial x \partial y = 0, \quad (1a)$$

where d/dt denotes the material derivative,

$$\bar{U} = U(y)\bar{e}_x, \quad d/dt = \partial/\partial t + U(y)\partial/\partial x, \quad (1b)$$

and c is the adiabatic sound speed, assumed to be constant. Since the mean flow properties do not depend on the time t or the longitudinal co-ordinate x , the acoustic pressure is conveniently represented by a Fourier integral in the time and the longitudinal co-ordinate:

$$P(x, y, t) = \int_{-\infty}^{+\infty} \int_{-\infty}^{+\infty} P(y; k, \omega) e^{i(kx - \omega t)} dk d\omega. \quad (2)$$

Here P is the pressure perturbation spectrum, for a wave of frequency ω and horizontal wavenumber k , at a distance y , say, from a wall. The dependence of the acoustic pressure on the transverse coordinate y is specified by substituting equation (2) into the acoustic wave equation in a shear flow (1a) leading to

$$P'' + \{2kU' / (\omega - kU)\}P' + \{(\omega - kU)^2 / c^2 - k^2\}P = 0, \quad (3)$$

where $U(y)$ is the velocity profile of the shear flow, and a prime denotes the derivative with respect to y : e.g., $P' \equiv dP/dy$, $P'' \equiv d^2P/dy^2$.

In the case of linear shear flow (see Figure 1), specified by the constant vorticity

$$q \equiv dU/dy = \text{const}; \quad U(y) = qy, \quad (4a, b)$$

the acoustic wave equation (3) takes the form

$$(\omega - qky)P'' + 2kqP' + (\omega - qky)\{(\omega - qky)^2/c^2 - k^2\}P = 0. \tag{5}$$

One of the approaches to the problem in the literature [19] is to use the change of variable:

$$\xi = \sqrt{2i/U'k}(\omega - kU)/c = \sqrt{2i/qk}(\omega - kqy)/c, \tag{6}$$

which places the origin at the layer of the zero Doppler shifted frequency:

$$\omega_*(y) \equiv \omega - kU(y) = \omega - kqy. \tag{7}$$

The layer of zero Doppler shifted frequency is known in wave theory as a critical layer [27–41, 65, 66], and in its vicinity ray theory breaks down. Note that a linear shear flow always has a critical layer, at $y_c = \omega/kq$, which appears as a singularity in the wave equation (5). Thus the physical interpretation of the change of independent variable (6) is that, apart from a multiplying factor, it places the origin at the critical layer for sound in a linear shear flow.

Besides the change of independent variable (6), a change of dependent variable [19] was used,

$$P = \{e^{b\xi^2/2}/(b + 1/2)\} d(e^{-b\xi^2/2}Q)/d\xi, \tag{8}$$

where $b \equiv k/2q$, leading to a third order differential equation for Q :

$$(d/d\xi)\{\xi^{-2} e^{-b\xi^2/2}[Q'' - (b + \xi^2/4)Q]\} = 0, \tag{9}$$

instead of a second order differential equation for P . Since the acoustic problem specifies two boundary conditions for the pressure P , the question arises of how to find three boundary conditions for the variable Q in equation (9). In other words, since there are three linearly independent solutions Q of equation (9), it is necessary to show that the transformation (8) leads to two linearly independent solutions for P . This issue is bypassed since in [19] what is solved is not the equation (9) in general, but the particular case in which the term in curly brackets vanishes:

$$Q'' + [(k/2q)^2 - \xi^2/4]Q = 0; \tag{10}$$

the nature of the singularity of equation (10) at $\xi = 0$ may be different from that of the singularity of equation (9) at $\xi = 0$. In fact equation (10) is devoid of

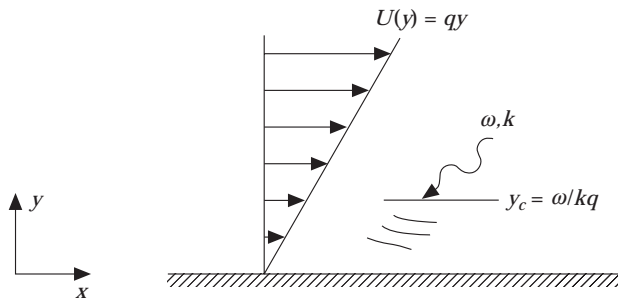


Figure 1. A linear shear flow, of constant vorticity q has a critical layer y_c for an incident acoustic wave of frequency ω and horizontal wavenumber k , where the Doppler shifted frequency vanishes.

singularities, whereas equation (9) has a regular singularity at $\xi = 0$. Thus although equation (10) is exactly solvable [19] in terms of parabolic cylinder functions, this (i) is not necessarily the general solution of the acoustic wave equation in a linear shear flow because of the restriction in passing from equation (9) to equation (10), and (ii) it may fail to represent accurately the sound field near the critical layer, because the critical layer $x = 0$ is a regular point of the differential equation (10) and a regular singularity of equation (9).

2.2. LOCATION OF THE CRITICAL LEVEL

This leads to a reconsideration of the problem of acoustic propagation in a linear shear flow (4a, b), starting from the wave equation (5). The critical layer is located at a distance $y = y_c$ from the wall such that the Doppler shifted frequency (7) vanishes,

$$\omega_*(y_c) = 0 \Leftrightarrow y_c = \omega/kq, \quad (11a, b)$$

suggesting the change of independent variable

$$\xi \equiv \omega_*(y)/\omega = 1 - (kq/\omega)y = 1 - y/y_c, \quad \Phi(\xi) = P(y, k, \omega), \quad (12a, b)$$

which places the critical layer at the origin $\xi_c = 0$ and the wall $y = 0$ at the point unity $\xi = 1$. The wall $y = 0$ is understood to be the line of zero mean flow velocity. The corresponding dependent variable (12b) satisfies a second order differential equation with polynomial coefficients of degree up to three,

$$\xi\Phi'' - 2\Phi' + \alpha\xi(\beta\xi^2 - 1)\Phi = 0, \quad (13)$$

where the prime denotes the derivative with respect to ξ , viz., $\Phi' \equiv d\Phi/d\xi$, and

$$\alpha \equiv (\omega/q)^2, \quad \beta \equiv (\omega/kc)^2 \quad (14a, b)$$

are dimensionless parameters.

The first dimensionless parameter (14a) is the square of the ratio of the wave frequency to the mean flow vorticity, i.e., is large for high frequency waves in weak vorticity, so that shear flow effects should be more important for small α . The second dimensionless parameter would be unity, $\beta = 1$, for acoustic propagation parallel to the mean flow $\omega = kc$, and greater than unity, $\beta > 1$, for oblique waves $\omega > kc$, in the case of ray theory, when a global dispersion relation would exist. The presence of the shear flow implies that the solution of the wave equation (5) is not sinusoidal in the y direction; hence there is no wavenumber in that direction, and no general dispersion relation. It is preferable to interpret the second dimensionless parameter (14b) as $\beta \equiv (u/c)^2$, the square of the ratio of the horizontal phase speed of the wave $u \equiv \omega/k$ to the sound speed c ; thus β is smaller, equal or larger than unity respectively for subsonic, sonic or supersonic horizontal phase speeds (by horizontal is meant parallel to the wall or the mean flow). Note that the horizontal phase speed always exists (1a), because the flow is uniform in the x direction.

The critical layer $\xi = 0$ is a regular singularity of the wave equation [61, 62]

$$\{1\}\xi^2\Phi'' + \{-2\}\xi\Phi' + \{\alpha\xi^2(\beta\xi^2 - 1)\}\Phi = 0, \quad (15)$$

because the terms in curly brackets are analytic functions of ξ , in the neighbourhood of $\xi = 0$. In fact they are analytic functions of ξ in the whole finite complex ξ -plane $|\xi| < \infty$, showing that the only other possible singularity of the differential equation (15) is the point at infinity: $\xi = \infty$. The behaviour of the solution at infinity is specified by the inverse variable near the origin,

$$\xi = 1/\eta, \quad \Psi(\eta) \equiv \Phi(\xi), \quad (16a, b)$$

viz., leading to the differential equation

$$\eta^2\Psi'' + 4\eta\Psi' + (\alpha/\eta)(\beta/\eta^2 - 1)\Psi = 0, \quad (17)$$

where the terms in curved brackets are singular at $\eta = 0$. Thus the singularity is irregular [59, 60] for the differential equation (17) at the origin $\eta = 0$: i.e., for the wave equation (13) at the point at infinity $\xi = \infty$.

2.3. REGULAR AND IRREGULAR SINGULARITIES

A differential equation with a regular singularity at the origin and an irregular singularity at infinity of degree one $0(1/\eta) \sim 0(\xi)$ may be reducible to the confluent hypergeometric type [67, 68], of which Weber's parabolic cylinder functions are a particular case. The singular coefficient is $0(1/\eta^3)$ in equation (17), and $0(\xi^3)$ in equation (13), which shows that the irregular singularity is of higher order, and reduction to a confluent hypergeometric equation is not immediate. It follows that these, or a particular case, like Weber's functions, may supply a solution of the problem only if a change of dependent variable is made. In fact, no further change of dependent variable is needed, because the wave equation (13) has two singularities only, at the origin and at the point at infinity, and the solution around either of these is valid in a region excluded by the order: i.e., it has an infinite radius of convergence. The solution around the point at infinity is more complicated, because the latter is an irregular singularity, and besides, it holds only for $|\xi| > 0$, and thus fails to converge at the critical layer.

This suggests the choice of the solution around the regular singularity at the origin, because (i) it specifies the acoustic field at the critical layer ($\xi = 0$ or $y = y_c$), and also in the whole flow region ($\xi < 1$ or $y > 0$), except at infinity ($y = \infty$ or $\xi = -\infty$), where the flow velocity itself diverges and (ii) the Frobenius-Fuchs method [59-62] can be applied: i.e., a solution exists as a power series

$$\Phi_\sigma(\xi) = \xi^\sigma \sum_{n=0}^{\infty} a_n(\sigma)\xi^n, \quad (18)$$

with index σ and a recurrence formula for the coefficients a_n to be determined. The latter is obtained by substituting equation (18) in equation (13), and equating to zero the coefficients of each power of ξ , viz.,

$$(n + \sigma)(n + \sigma - 3)a_n(\sigma) = \alpha a_{n-2}(\sigma) - \alpha\beta a_{n-4}(\sigma). \quad (19)$$

Note that this recurrence formula is quickly convergent for large n , because the coefficient of a_n is $0(n^2)$, and the coefficients of a_{n-2} , a_{n-4} are $0(1)$: i.e., successive iterations behave like $0(1/n^2)$. The appearance of the term a_{n-4} is due to the high order of the irregular singularity at infinity.

Setting $n = 0$ in the recurrence relation (19) yields

$$\sigma(\sigma - 3)a_0(\sigma) = 0. \tag{20}$$

Note that $a_0 \neq 0$, otherwise by equation (19) all $a_n = 0$, leading to a trivial solution $\Phi = 0$ in equation (18). Thus equation (20) leads to the indicial equation $\sigma(\sigma - 3) = 0$, showing that the two possible values of the index $\sigma_1 = 3$, $\sigma_2 = 0$, differ by an integer $\sigma_1 - \sigma_2 = 3$. The recurrence formula (19) holds for $n \geq 4$, and for smaller values simplifies to

$$\begin{aligned} (\sigma + 1)(\sigma - 2)a_1(\sigma) &= 0, & (\sigma + 2)(\sigma - 1)a_2(\sigma) &= \alpha a_0(\sigma), \\ (\sigma + 3)\sigma a_3(\sigma) &= \alpha a_1(\sigma), \end{aligned} \tag{21a-c}$$

since $0 = a_{-1}(\sigma) = a_{-2}(\sigma) = \dots$ because the corresponding negative powers are absent from the Frobenius–Fuchs series expansion (18). The latter, together with equations (19, 20, 21a–c) suffice to determine two linearly independent solutions, corresponding to the two values $\sigma_1 = 3$ and $\sigma_2 = 0$ of the index.

3. PAIR OF LINEARLY INDEPENDENT SOLUTIONS

The linearly independent solutions are functions which are even and odd relative to the critical layer, and can be used to demonstrate the effects of frequency and wavenumber, in the case of real waveforms.

3.1. DECOMPOSITION INTO EVEN AND ODD FUNCTIONS

For the index $\sigma_1 = 3$, the coefficients of odd order in equations (21a), (21c) and (19) all vanish,

$$\sigma_1 = 3: \quad 0 = a_1(3) = a_3(3) = \dots = a_{2n+1}(3), \tag{22}$$

leaving as potentially non-zero only the even coefficients; $a_0(3)$ in equation (20) in arbitrary because $0a_0 = 0$, and the remaining coefficients of even order are related to a_0 (21b), (19) by

$$\sigma_1 = 3: \quad 10a_2(3) = \alpha a_0(3), \quad 2n(2n + 3)a_{2n}(3) = \alpha[a_{2n-2}(3) - \beta a_{2n-4}(3)]. \tag{23a, b}$$

The non-zero coefficients may be redesignated as

$$b_n \equiv a_{2n}(3): \quad 10b_1 = \alpha b_0, \quad 2n(2n + 3)b_n = \alpha(b_{n-1} - \beta b_{n-2}), \tag{24a, b}$$

and they specify a solution (18) as

$$\Phi_3(\xi) = \sum_{n=0}^{\infty} a_{2n}(3)\xi^{2n+3}, \tag{25a}$$

which is an odd function

$$b_0 \equiv 1: \quad F(\xi) \equiv \sum_{n=0}^{\infty} b_n \xi^{2n+3} = -F(-\xi), \tag{25b}$$

of the distance from the critical layer.

Concerning the other index $\sigma_2 = 0$, it follows from equation (21c) that $0a_3(0) = 0$, so that $a_3(0)$ is arbitrary. If it is assumed that it is non-zero, then upon starting with $a_3(0) \neq 0$, the recurrence formula (19) leads again to the preceding solution (25a), within a constant multiplying factor. Since the aim is to obtain a solution which is linearly independent of equation (25a), there is no loss of generality in setting $a_3(0) = 0$. Since for $\sigma_2 = 0$ it follows from equation (21a) that $a_1(0) = 0$, then all coefficients of odd order vanish,

$$\sigma_2 = 0: \quad 0 = a_1(0) = a_3(0) = \dots = a_{2n+1}(0), \tag{26}$$

as in equation (22). From equation (20) it follows that $0a_0(0) = 0$, so that $a_0(0)$ is arbitrary, and a non-zero value $a_0(0) \neq 0$ is necessary to avoid a trivial solution; the remaining coefficients of even order are related to $a_0(0)$ by equations (21a) and (19):

$$\sigma_2 = 0: \quad -2a_2(0) = \alpha a_0(0), \quad 2n(2n - 3)a_{2n}(0) = \alpha[a_{2n-2}(0) - \beta a_{2n-4}(0)]. \tag{27a, b}$$

Upon redesignating the coefficients

$$d_n \equiv a_{2n}(0): \quad -2d_1 = \alpha d_0, \quad 2n(2n - 3)d_n = \alpha(d_{n-1} - \beta d_{n-2}), \tag{28a, b}$$

these specify a solution (18)

$$\Phi_0(\xi) = \sum_{n=0}^{\infty} a_{2n}(0) \xi^{2n}, \tag{29a}$$

which is an even function

$$d_0 \equiv 1: \quad G(\xi) \equiv \sum_{n=0}^{\infty} d_n \xi^{2n} = G(-\xi), \tag{29b}$$

of the distance from the critical layer, and hence linearly independent of the solution specified by equations (25a, b).

3.2. EFFECTS OF FREQUENCY AND WAVENUMBER

The decomposition of the wave field into functions which are respectively even (29b) and odd (25b) relative to the critical layer has arisen naturally from the application of the Frobenius–Fuchs method to the wave equation; the existence of this decomposition has been overlooked in the literature, due to the use of further changes of variable, which are necessary to reduce the problem to known

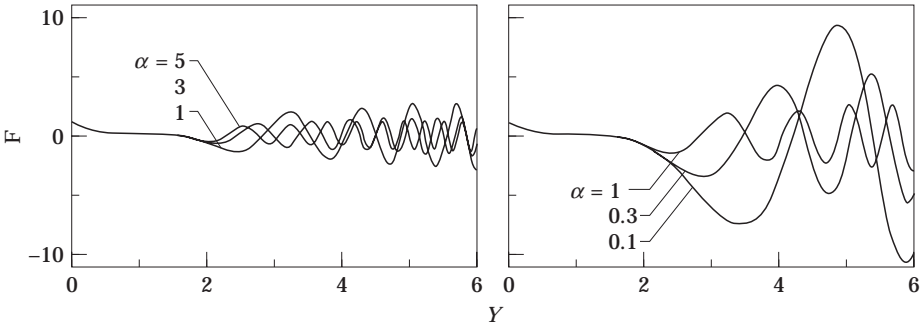


Figure 2. Part of the acoustic pressure spectrum which is (25b; 24a, b) an odd function of dimensionless distance from the critical layer, plotted as function of the dimensionless distance from the wall for a range (31b) of six critical layer distances; effect of varying the ratio of wave frequency to mean flow vorticity (14a), while keeping fixed the ratio of horizontal phase speed to sound speed. $\beta = 5$.

special functions. This decomposition shows that the two functions are linearly independent, and hence that the general integral of equation (13) is a linear combination of equations (25b) and (29b):

$$P(y; k, \omega) = AF(1 - Y) + BG(1 - Y), \quad Y \equiv y/y_c = 1 - \xi, \quad (30a, b)$$

where Y (30b) is (12a) the distance from the wall, made dimensionless by dividing by the distance from the critical layer. The constants of integration A, B are determined from boundary conditions. Note in passing that b_0 in equation (25b) and d_0 in equation (29b) can be incorporated respectively in the arbitrary constants A and B , and thus there is no loss of generality in setting $b_0 \equiv 1 \equiv d_0$.

Since different pairs of boundary conditions give different values of A, B , it is preferable to plot separately the two components of the solution, to illustrate the decomposition of the general wave field in components symmetric G and skew-symmetric F relative to the critical layer, which is the main feature of the present paper distinguishing it from the preceding literature. The acoustic fields are plotted versus dimensionless distance from the critical layer (12a) or from the wall (30b),

$$-5 \leq \xi \leq 1, \quad 0 \leq Y \equiv y/y_c \leq 6, \quad (31a, b)$$

covering a range of distances from the wall equal to six times the distance of the critical layer. The odd F (25b; 24a, b) and even G (29b; 28a, b) components of the general acoustic field (30a), are plotted separately, respectively in Figures 2–5. There are two dimensionless parameters (14a, b), to which the following reference values are given,

$$\alpha = 1, \quad \beta = 5, \quad (32a, b)$$

corresponding respectively to a wave frequency equal to the vorticity $\omega = q$, and an horizontal wavenumber $k\sqrt{5} = \omega/c$; in the ray limit, in the absence of mean flow, this corresponds to a transverse wavenumber $K = \sqrt{(\omega/c)^2 - k^2} = 2k$ twice

the horizontal wavenumber: i.e., propagation at an angle $\theta = \arctan(K/k) = \arctan 2 = 63.4^\circ$ to the mean flow direction, which is horizontal. In Figure 4 (2) for the even (odd) function, the parameter β is kept fixed at (32b), and α takes the values

$$\alpha = 0.1, 0.3, 1, 3, 5, \quad (33)$$

ranging from wave frequencies lower than, to higher than, the vorticity; in Figure 5 (3) for the even (odd) function, α is kept fixed at (32a), and β takes the values

$$\beta = 1, 3, 5, 7, 10, \quad (34)$$

ranging from the ray limit to a transverse wavenumber from zero to three times the horizontal wavenumber.

3.3. SUPPRESSION OF OSCILLATORY BEHAVIOUR

Concerning the odd function, and variations of the first parameter, it has long oscillations with large amplitude for small frequency or large vorticity (Figure 2, r.h.s.), and short oscillations of small amplitude for high frequency or small vorticity (Figure 2, l.h.s.). The same trend applies to the odd function and variations of the second parameter; i.e., (Figure 3), as the frequency increases or horizontal wavenumber decreases, the oscillations reduce in amplitude and the nodes are closer. Concerning the even function, the effects are different for the first parameter, viz., as frequency increases or vorticity decreases the oscillation amplitude increases and the nodes become more closely spaced; this contrast is shown by the plots (in Figure 4) of the largest and smallest values of the parameter (r.h.s.) and the three intermediate values (l.h.s.). Also concerning the even function, and the dependence on the second parameter, the behaviour is less markedly different (Figure 5) from the odd function; as frequency increases or horizontal wavenumber increases, the amplitude of the oscillation decreases and the nodes become closer, although less markedly so than before.

The separate plots of the even and odd parts of the acoustic field as functions of the dimensionless distance from the wall, for various values of the two dimensionless parameters, show a number of common features: (i) the oscillations tend to grow in amplitude towards infinity, as the flow velocity diverges at large distance for a linear velocity profile; (ii) the spacing of the nodes increases as the critical layer is approached; (iii) in the vicinity of the critical layer there are no oscillations at all, for the odd component vanishes, and the even component is unity; (iv) the acoustic field does not vary much between the critical layer and the wall, and large or marked oscillations occur only into the stream far from the critical layer. Thus the critical layer acts such as to suppress oscillations in its vicinity.

4. CASES WITH COMPLEX WAVEFUNCTION

By allowing the wall to be at a variable distance from the critical layer, instead of distance unity, it is possible to reduce the problem to a single parameter. This simplifies the representation of real waveforms, and is also convenient for complex

wave fields; the latter may arise from a complex wavenumber or from other boundary conditions, e.g., of impedance type.

4.1. COMPLEX WAVENUMBER AND STABILITY

The preceding solutions may be considered with a complex wavenumber:

$$k = k_r + ik_i; \quad e^{ikx} = \exp(ik_r x) \exp(-k_i x). \quad (35)$$

In this case (2) the real part k_r acts as the wavenumber, and the imaginary part k_i indicates the stability of the linear shear flow with regard to acoustic disturbances, viz: (i) if $k_i > 0$ they are exponentially damped (stability); (ii) if $k_i < 0$ they grow in space (instability); (iii) if $k_i = 0$ their amplitude is constant (neutral stability). Note that the preceding corresponds to the study of stability in space, starting from a real frequency ω (it would be possible to do the reverse, i.e., study stability in time, with real k and complex ω). For this spatial stability approach, the parameter α is real (14a), and the change of independent variable

$$\zeta \equiv \alpha \zeta = (\omega/q)^2(1 - y/y_c) = (\omega/q)^2 - \omega k y/q, \quad \Theta(\zeta) \equiv \Phi(\zeta) = P(y; k, \omega), \quad (36a, b)$$

transforms the wave equation (13) to

$$\zeta \Theta'' - 2\Theta' + \zeta(\gamma \zeta^2 - 1)\Theta = 0, \quad (37)$$

which involves a dimensionless parameter

$$\gamma \equiv \beta/\alpha^2 = [q^2/(kc\omega)]^2. \quad (38)$$

The change of independent variable (36a) keeps the critical layer at the origin ($\zeta = 0$ for $y = y_c$), but places the wall at variable distance from it $\zeta = (\omega/q)^2 = \alpha$ for $y = 0$.

The parameter (38) is real for real wavenumber, and complex for complex wavenumber; in the latter case the critical layer is at a real position (11b) for the real frequency. In the case of complex frequency, the critical layer would be at a complex position (11b). This feature is not uncommon, for other types of waves, e.g., non-dissipative magnetosonic-gravity waves have a critical layer at a “real” altitude [36, 38, 69], and viscous and resistive Alfvén waves have a critical layer at complex “altitude” [37, 39, 40, 66]. The meaning of a critical layer at a real co-ordinate (or altitude) is that the wave equation has a regular singularity at this point, with exponent σ , so that if (i) $\text{Re}(\sigma) > 0$ the wave field vanishes at the critical layer, (ii) if $\text{Re}(\sigma) < 0$ the wave field is singular at the critical layer, (iii) if $\text{Re}(\sigma) = 0$ the wave field is finite and non-zero at the critical layer. For example, in the present problem of sound propagation, with real wavenumber k , in a linear shear flow, of the preceding three cases, two occur: (a) the index $\sigma_1 = 3$, corresponds to a wave field (25b) which is an odd function of the distance from the critical layer, and thus vanishes there (case (i) above with $\text{Re}(\sigma_1) = 3 > 0$); (b) the index $\sigma_2 = 0$, corresponds to a wave field (29b) which is an even function of the distance from the critical layer, and is finite and non-zero there (case (iii) above with $\text{Re}(\sigma_2) = 0$). In the case of a critical layer at a complex co-ordinate (or

altitude), the wave field is finite at all positions (i.e., on the real axis), because there is no singularity there. The critical layer at a complex co-ordinate may still limit the radius of convergence of a power series solution about another point. However, in the present problem, the only other singularity of the wave equation is the point at infinity. Thus when expanding in power series about the critical layer, the radius of convergence is infinite, regardless of where the critical layer is, i.e., whether it is at real or complex position. Thus the preceding solutions hold equally well for real or complex wavenumber. The odd solution is (25b; 24a, b) thus

$$H(\zeta) = \sum_{n=0}^{\infty} f_n \zeta^{2n+3} = \sum_{n=0}^{\infty} f_n [(\omega/q)^2(1 - Y)]^{2n+3} = -H(-\zeta), \tag{39a}$$

with the recurrence formula for the coefficients being

$$f_0 = 1, f_2 = 1/10; \quad 2n(2n + 3)f_n = f_{n-1} - \gamma f_{n-2}; \tag{39b}$$

the even function (29b; 28a, b) is similarly:

$$J(\zeta) = \sum_{n=0}^{\infty} g_n \zeta^{2n} = \sum_{n=0}^{\infty} g_n [(\omega/q)^2(1 - Y)]^{2n} = J(-\zeta), \tag{40a}$$

with the recurrence formula for the coefficients being

$$g_0 = 1, g_1 = -1/2; \quad 2n(2n - 3)g_n = g_{n-1} - \gamma g_{n-2}. \tag{40b}$$

The two components of the wavefield, viz., odd (39a, b) and even (40a, b) may be illustrated for real or complex wavenumber in terms of equation (38), the only remaining parameter γ .

The choice of parameters for equation (33) dimensionless frequency $0.1 \leq \alpha \leq 5$ and equation (34) dimensionless wavenumber $1 \leq \beta \leq 10$ would lead, for the single parameter (38), to $0.04 = 1/25 \leq \gamma \leq 1000$, a very wide range of values. For a real wavevector, a more modest range of values of γ is chosen,

$$\gamma = 0.5, 1, 2, 8, \tag{41}$$

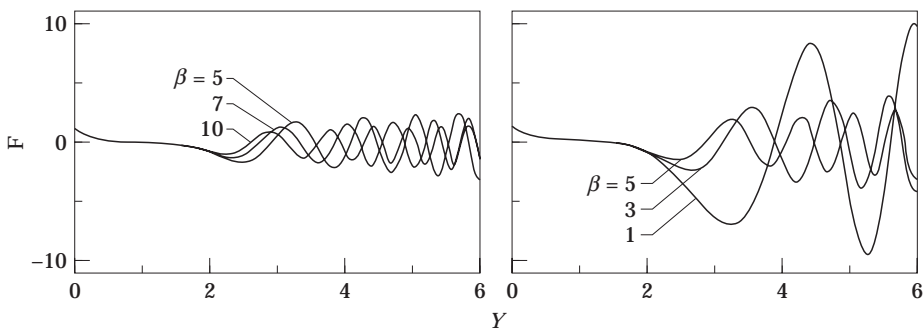


Figure 3. As for Figure 2: effect of varying the ratio of horizontal phase speed to sound speed (14b), while keeping fixed the ratio of wave frequency to vorticity. $\alpha = 1$.

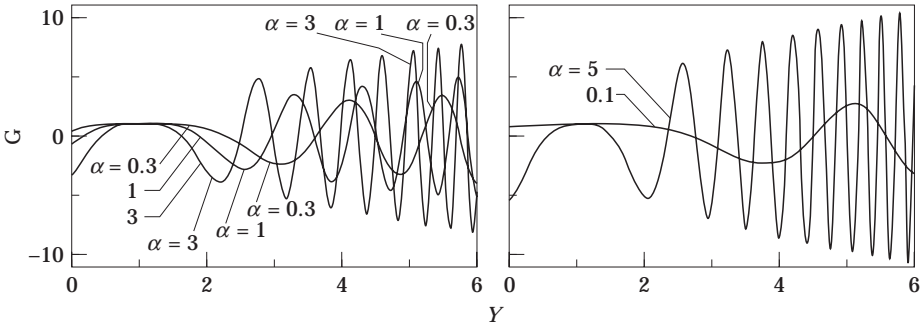


Figure 4. Part of the acoustic field which is (29b; 28a, b) an even function of the dimensionless distance from the critical layer, plotted as a function of the dimensionless distance from the wall for a range of six critical layer distances; effect of changing the ratio of wave frequency to mean flow vorticity, and keeping fixed the ratio of horizontal phase speed to sound speed. $\beta = 5$.

for plotting of the odd H (Figure 6) and even J (Figure 7) wave fields, versus the dimensionless variable ζ (36a), measuring distance from the critical layer $\zeta = 0$. Note that the parameter γ equals (38) the square of the ratio q/ω of vorticity to frequency multiplied by the ratio q/kc of vorticity to “frequency” calculated for horizontal propagation. Thus γ is larger for stronger vorticity and lower frequency and horizontal wavenumber. The odd wavefield H remains small (Figure 6) between the wall and the critical layer, and towards the free stream, the acoustic field diverges, sooner for larger γ and with larger amplitude for smaller γ . The even wavefield J decays from the critical layer to the wall (Figure 7), more for larger γ ; it is unity at the critical layer, and it diverges towards the free stream, as before sooner for larger γ and with larger amplitude for smaller γ . The case of complex γ would give rise to complex wavefields; the latter also arise for impedance boundary conditions, which are considered next.

4.2. CHOICE OF BOUNDARY CONDITIONS

The general wave field is again a linear combination of odd (39a, b) and even (40a, b) solutions,

$$P(y; k, \omega) = CH(\alpha(1 - Y)) + DJ(\alpha(1 - Y)), \tag{42}$$

where C, D are arbitrary constants, specified by two independent, and compatible boundary conditions. These could be (i) the acoustic pressure at two points in the flow:

$$P(y_1; k, \omega) = P_1, \quad P(y_2; k, \omega) = P_2. \tag{43a, b}$$

The acoustic pressure p and the vertical velocity V_y , are related by the y -component of the linearized momentum equation,

$$-\rho^{-1} \partial p / \partial y = dv_y / dt = \partial v_y / \partial t + U(y) \partial v_y / \partial x, \tag{44}$$

where ρ is the mass density of the mean flow; using the spectra of the pressure (2) and acoustic velocity,

$$v_y(x, y, t) = \int_{-}^{+} \int_{\infty}^{\infty} V_y(y; k, \omega) e^{i(kx - \omega t)} dk d\omega, \tag{45}$$

leads to the polarization relation

$$dP(y; k, \omega)/dy = i\rho[\omega - kU(y)]V_y(y; k, \omega). \tag{46}$$

Thus another set of boundary conditions, would be to specify (ii) the acoustic pressure and transverse velocity, at the same point in the flow:

$$P(y_1; k, \omega) = P_1, \quad V_1 = -iP'(y_1; k, \omega)/\{\rho[\omega - kU(y_1)]\}. \tag{47a, b}$$

A combination of (iii) acoustic pressure and velocity at different points, e.g., equations (43b) and (47b), would also do as a two-point boundary value problem. One of the boundary conditions could be replaced by a boundary condition at the wall. At the wall $y = 0$, the free stream velocity vanishes $U(0) = 0$, so that the polarization relation (46) between acoustic velocity and pressure reduces to that for a fluid at rest:

$$V_y(0; k, \omega) = -(i/\rho\omega)P'(0; k, \omega). \tag{48}$$

Assuming a wall with impedance Z ,

$$P(0; k, \omega) = ZV_y(0; k, \omega), \tag{49a}$$

leads to the boundary condition (iv)

$$P(0; k, \omega) + i(Z/\rho\omega)P'(0; k, \omega) = 0, \tag{49b}$$

which is of third kind or mixed type. In the particular case of a rigid wall, i.e., infinite impedance (v),

$$Z = \infty: \quad P'(0; k, \omega) = 0, \tag{50}$$

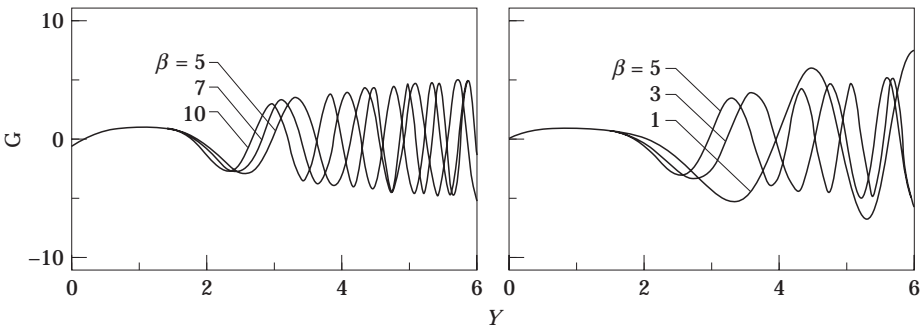


Figure 5. As for Figure 4: Effect of varying the ratio of horizontal phase speed to sound speed, while keeping fixed the ratio of wave frequency to mean flow vorticity. $\alpha = 1$.

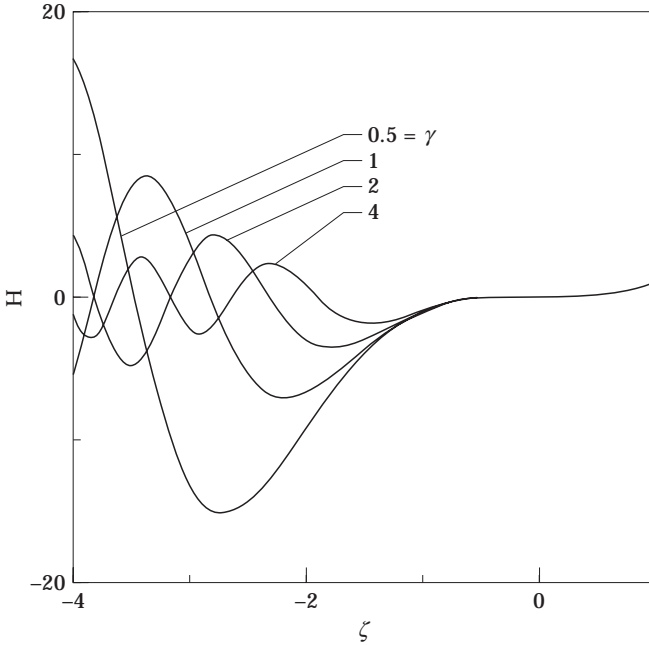


Figure 6. As for Figures 2 and 3, the acoustic pressure spectrum which is (39a, b) an odd function of the distance from the critical layer, is plotted versus modified dimensionless distance (36a, 14a), for four values of the dimensionless parameter (38) combining vorticity, wave frequency and wavenumber.

the normal derivative of the acoustic pressure vanishes, because the normal acoustic velocity is zero. The boundary condition is replaced by

$$-(i/\rho\omega)P'(0; k, \omega) = V_0(k, \omega), \tag{51}$$

for (vi) a moving wall with prescribed normal velocity spectrum.

If the linear shear flow is matched to an uniform stream of velocity U_∞ ,

$$U(y) = \begin{cases} qy & \text{if } y \leq L, \\ qL \equiv U_\infty & \text{if } y \geq L, \end{cases} \tag{52}$$

to simulate a boundary layer of thickness L , then one boundary condition can be applied at infinity, e.g., a (vii) radiation condition, specifying an inward ($-$ sign) or outward ($+$ sign) propagating wave,

$$\text{as } y \rightarrow \infty: \quad P(y; k, \omega) \sim e^{\pm iKy}, \tag{53a}$$

where

$$K = |(\omega - kqL)^2/c^2 - k^2|^{1/2}, \tag{53b}$$

is the transverse wavenumber in the free stream $U(\infty) = qL$. In the case of an unbounded linear shear flow (4b), another possible boundary condition (viii)

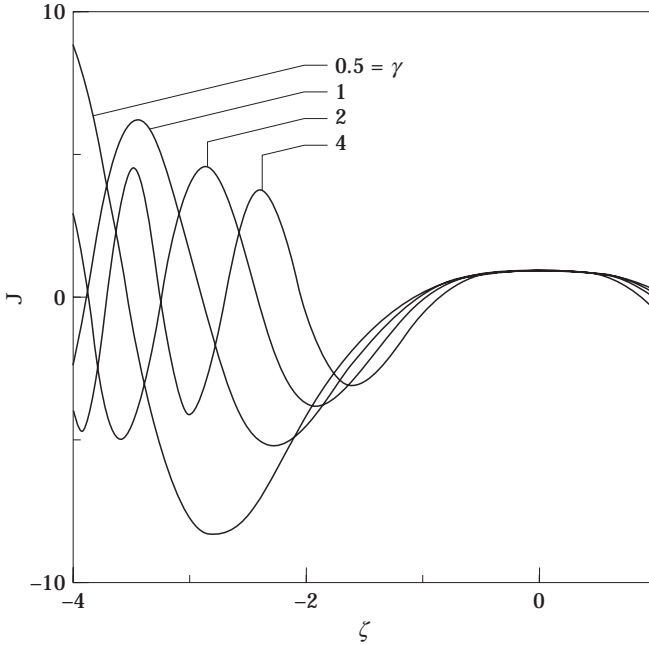


Figure 7. As for Figure 6, for the acoustic pressure spectrum which is (40a, b) an even function of distance from the critical layer.

specifies the acoustic pressure at the critical layer, which determines the constant of integration D in equation (42),

$$P_c(k, \omega) \equiv P(y_c; k, \omega) = D, \tag{54}$$

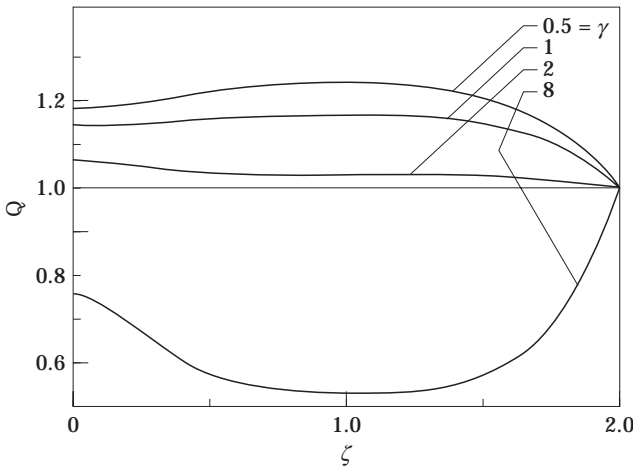


Figure 8. Total acoustic pressure spectrum (42), normalized (60a) to the value at a distance (60b), plotted versus modified dimensionless distance (36a), for four values (41) of dimensionless parameter (38), in the case of a rigid wall (50).

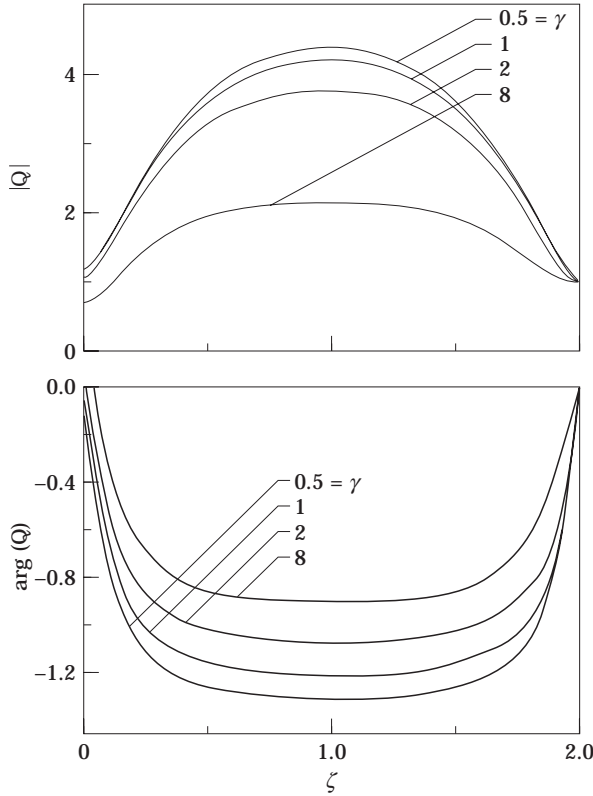


Figure 9. As for Figure 8, for a compliant wall with specific impedance $z \equiv Z/\rho c = 0.1$, with separate plots for amplitude (top) and phase (bottom).

because the odd solution $H(\zeta)$ vanishes (39a) at the critical layer $H(0) = 0$, and the even solution $J(\zeta)$ is (40a) unity $J(0) = g_0 \equiv 1$.

Most boundary conditions specify a relation between C and D ; in equation (42) e.g., (iv) the moving wall condition (51),

$$i(\rho q/k)V_0(k, \omega) = CH'(\alpha) + DJ'(\alpha), \tag{55}$$

where the prime denotes the derivative $H' \equiv dH/d\zeta$ with regard to ζ in equation (36a). Solving equations (54) and (55) for C, D and substituting in equation (42), leads to a first example (a) of the explicit acoustic pressure,

$$P(y; k, \omega) = P_c(k; \omega)J(\alpha(1 - Y)) - [i(\rho q/k)V_0(k; \omega) + P_c(k; \omega)J'(\alpha)]\{H(\alpha(1 - Y))/H'(\alpha)\}, \tag{56}$$

for the boundary conditions (vi), (viii). As another example (b), the impedance wall condition (49b), applied to equation (42) yields

$$\chi \equiv kZ/\rho q: \quad CH(\alpha) + DJ(\alpha) = i\chi[CH'(\alpha) + DJ'(\alpha)]; \tag{57}$$

together with equation (54), this shows that the acoustic pressure field which satisfies the boundary conditions (iv; viii) is specified by

$$P(y, k, \omega) = P_c(k, \omega) \{ H(\alpha(1 - Y)) - J(\alpha(1 - Y)) \times [J(\alpha) - i\chi J'(\alpha)] / [H(\alpha) - i\chi H'(\alpha)] \}. \tag{58}$$

A particular case (c) is that of a rigid wall (50), i.e., the acoustic field satisfying (v, viii) is given by

$$Z = \infty; \quad P(y; k, \omega) = P_c(k, \omega) \{ H(\alpha(1 - Y)) - [J'(\alpha)/H'(\alpha)] J(\alpha(1 - Y)) \}, \tag{59}$$

which corresponds to the limit $\chi \rightarrow \infty$ taken in equation (58).

4.3. AMPLITUDE AND PHASE VARIATIONS

As an example of the use of the preceding boundary conditions, the acoustic pressure

$$Q(Y) \equiv P(y; k, \omega) / P(y_2; k, \omega), \quad y_2 = y(\zeta = 2) = y_c(1 - 2/\alpha), \tag{60a, b}$$

normalized to the value (36a) at $\zeta = 2$, i.e., $y_* = y_c(1 - 2/\alpha)$, in equation (60b) is plotted for the same values (41) of the parameter γ as before (Figures 6 and 7), but this time for the total acoustic field with (Figure 8) a rigid wall (impedance $Z = \infty$), leading to a real wave field, (Figure 9) a compliant wall of specific impedance $z \equiv Z/\rho c = 0.1$, requiring separate plots of $|Q|$ amplitude (top) and $\arg(Q)$ (bottom).

In the case of a rigid wall (Figure 8) the pressure increases towards the wall, for intermediate values of $\gamma = 2$, and it decreases for small $\gamma = 0.5$, i.e., (38) for weak vorticity, high frequency or large wavenumber. As γ increases, (e.g., $\gamma = 8$),

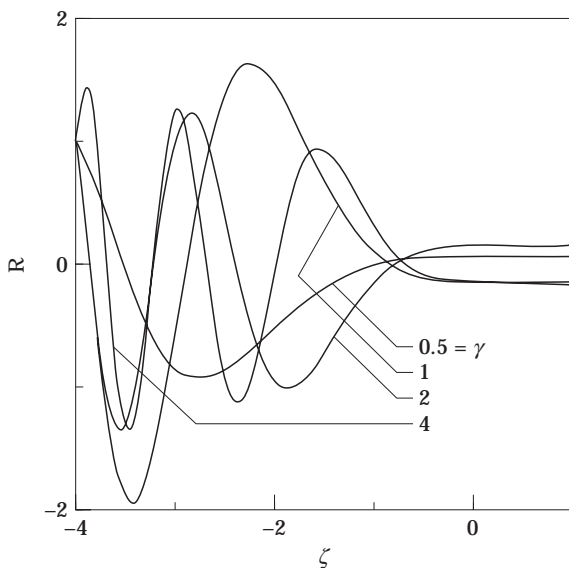


Figure 10. Total acoustic pressure spectrum (42), normalized (61a) to the value at a distance (61b), versus modified dimensionless distance (36a), for four values (62) of the dimensionless parameter (38), and a rigid wall.

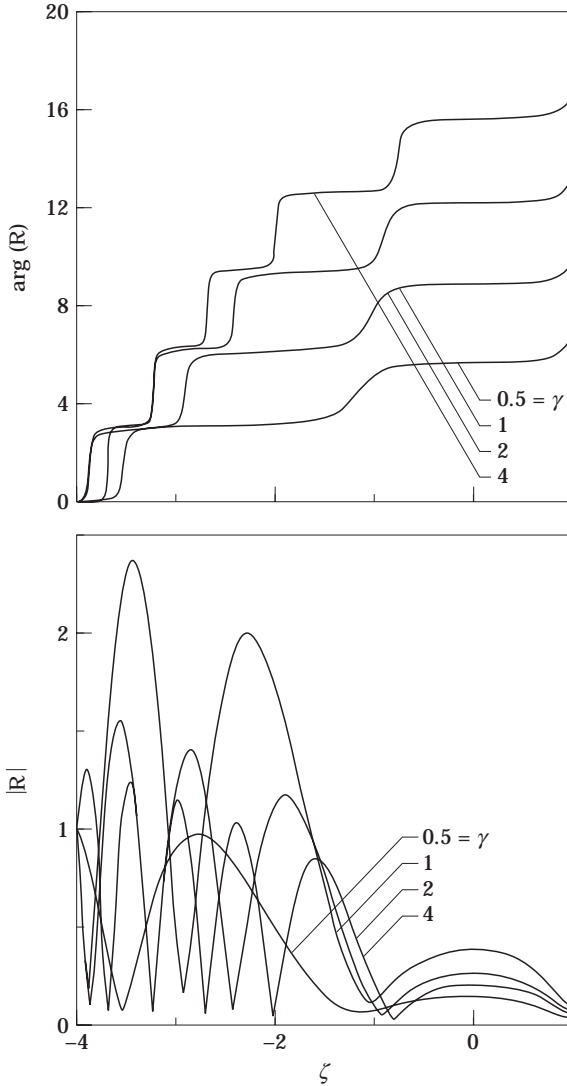


Figure 11. As for Figure 10, for a wall of specific impedance $z = 0.1$, leading to a complex wavefield, with separate plots of amplitude (bottom) and phase (top).

i.e., for strong vorticity or low frequency or small wavenumber, the acoustic pressure reverses from compression to depression. For large or small values of γ the acoustic pressure has an extremum at the critical layer, e.g., a maximum for $\gamma \leq 1$ and a minimum for $\gamma = 8$; the critical layer is not an extremum of the acoustic pressure for intermediate values of γ e.g., $\gamma = 2$.

In the case of a compliant wall (Figure 9), with specific impedance $z \equiv Z/\rho c = 0.1$, the modulus of the acoustic pressure (top), shows that it is again maximum at the critical layer, with the value of the maximum decreasing as γ increases, i.e., for stronger vorticity, lower frequency or smaller wavenumber; the amplitude thus decays towards the wall, where it is smaller for increasing γ . The phase (bottom) varies little near the critical layer, in agreement with the earlier

finding that the latter tends to suppress oscillations (section 3.3). Most of the phase changes occur near to the wall, and near to the point $\zeta = 2$ of imposed pressure, with a faster variation for smaller γ , i.e., weaker vorticity, higher frequency or larger wavenumber; these thus lead to larger absolute values of the negative phase at its extremum (or minimum) near the critical layer $\zeta = 0$.

The next plot concerns also a wall of specific impedance $z = Z/\rho c = 0.1$, but the acoustic pressure is normalized (61a) as

$$R(Y) = P(y; k, \omega)/P(y_4; k, \omega), \quad y_4 \equiv y(\zeta = -4) = y_c(1 + 4/\alpha), \tag{61a, b}$$

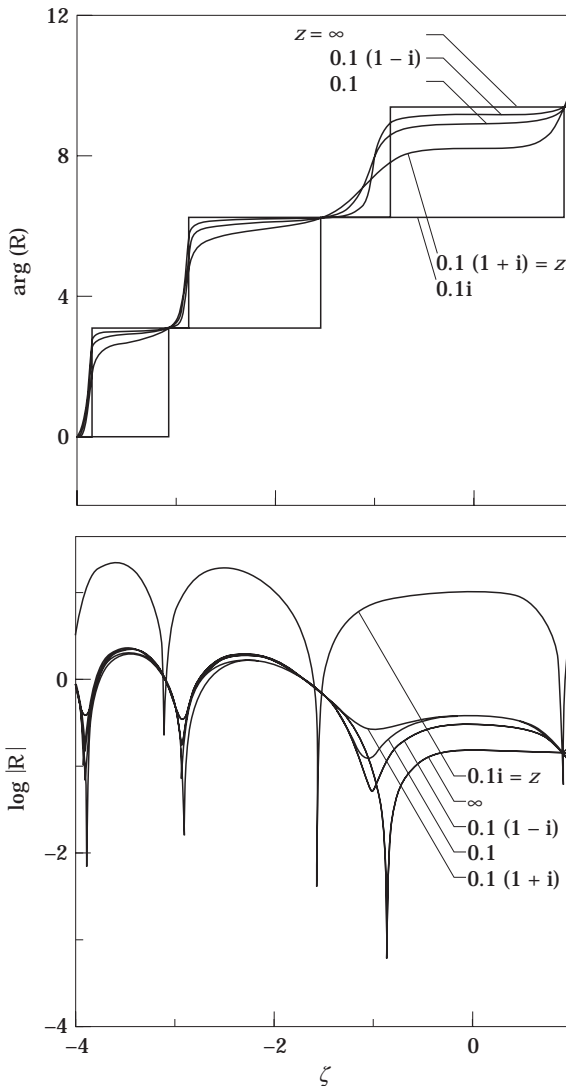


Figure 12. As for Figure 11, with fixed $\gamma = 1$, and several values of wall impedance (63), viz., rigid wall $z = \infty$, capacitive wall, $z = 0.1i$, active wall $z = 0.1$, and resistive wall $z = 0.1(1 \pm i)$.

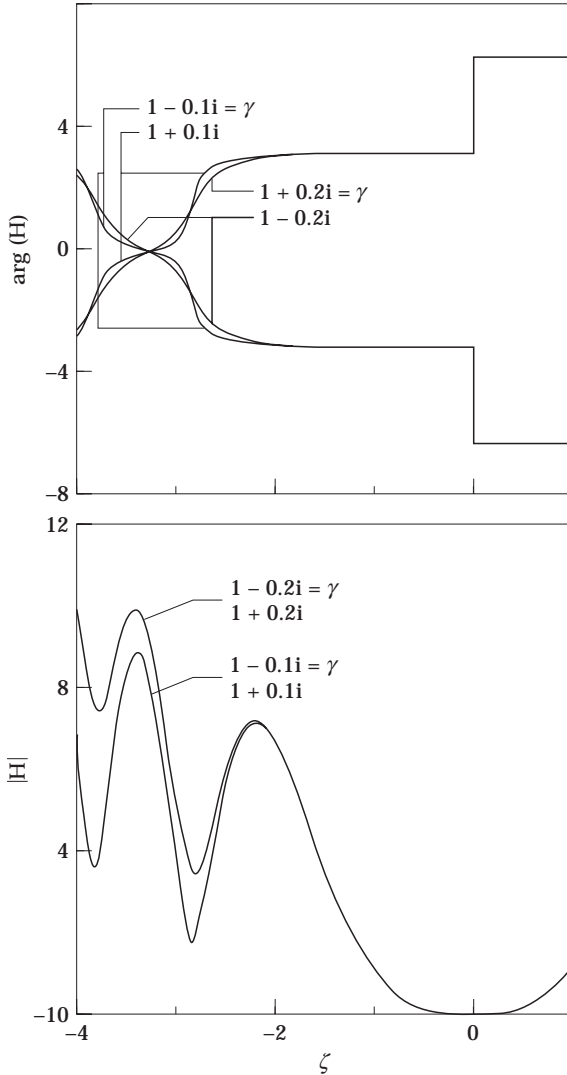


Figure 13. Acoustic pressure spectrum which is (39a, b) an even function of distance from the critical layer, plotted versus modified dimensionless distance from the critical layers (36a), for complex values (64) of dimensionless parameters (38), separating amplitude (bottom) and phase (top).

to the value at $\zeta = -4$ or (61b). The acoustic pressure field, for four real values

$$\gamma = 0.5, 1, 2, 4, \quad (62)$$

of the parameter (38), is real for a rigid and complex for an impedance wall. In the case of a rigid wall, the real wave field (Figure 10) varies little near the critical layer $\zeta = 0$ and towards the wall $\zeta > 0$, and oscillates towards the free stream. A wall with specific impedance $z = 0.1$ leads to a complex wave field (Figure 11) requiring separate plots of modulus or amplitude (bottom) and argument or phase (top). The amplitude (bottom) has a maximum near the critical layer $\zeta = 0$, and decays towards the wall $\zeta > 0$; towards the free stream $\zeta < 0$ there are diverging

oscillations. At the zeros of the acoustic pressure (bottom), or nodes of the waveform, there are phase jumps of π (top), between which the phase does not vary much; thus the phase of the acoustic field looks like a “staircase” function, with rounded-off phase jumps of π at the nodes of the wave form.

With the same normalization for the acoustic pressure (61a, b), but with the parameter fixed at $\gamma = 1$, several values of the wall specific impedance are considered,

$$\gamma = 1; \quad z \equiv Z/\rho c = \infty, 0.1, i0.1, 0.1(1 \pm i), \quad (63)$$

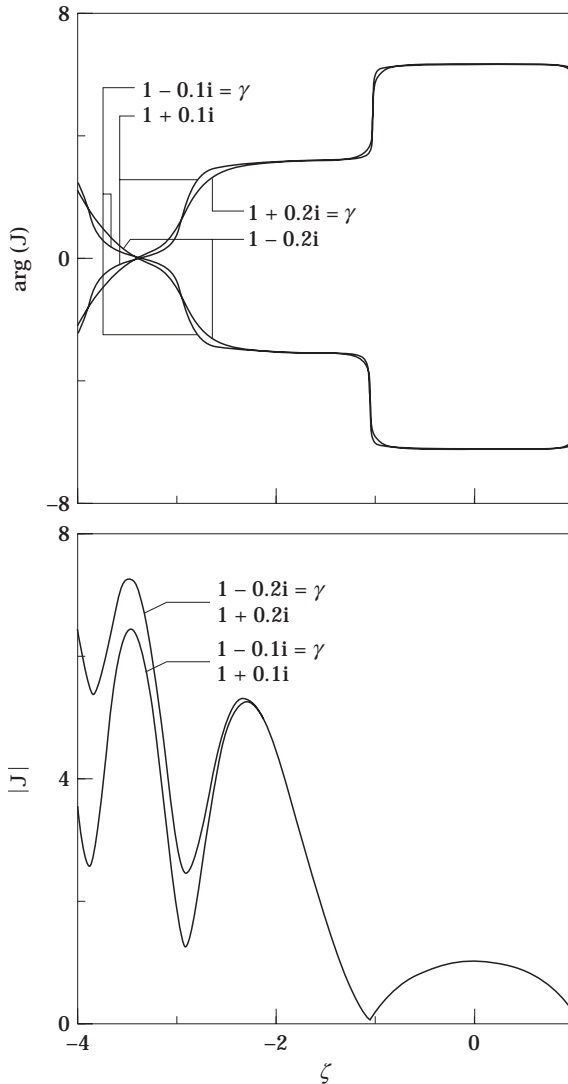


Figure 14. As for Figure 13, for an acoustic pressure spectrum which is (40a, b) an odd function of distance from the critical layer.

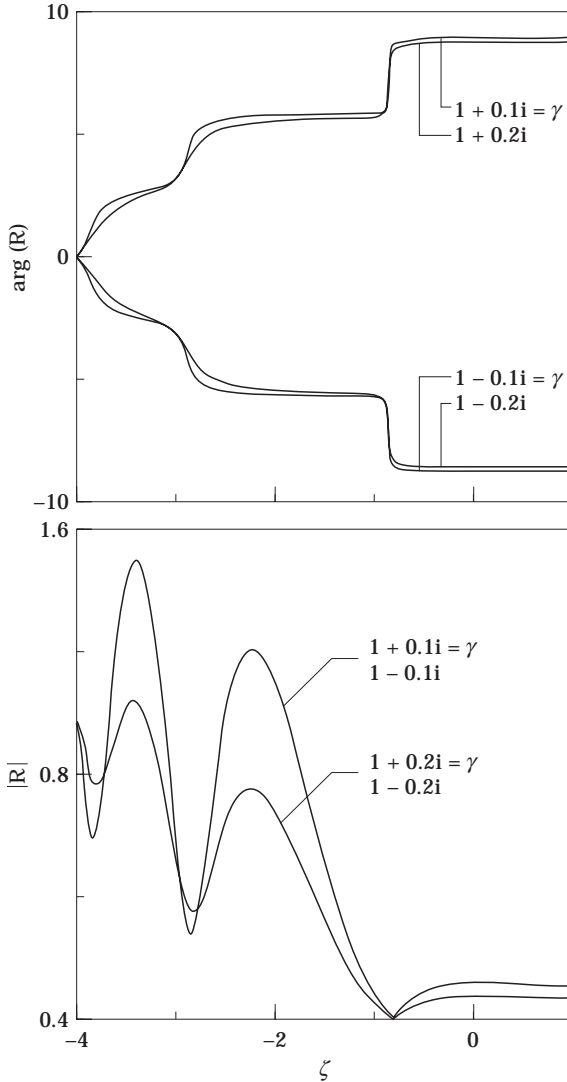


Figure 15. Total acoustic pressure spectrum (42), normalized (61a) to the value at a distance (61b), versus modified dimensionless distance (36a), for a rigid wall and for four values (63) of the dimensionless parameter (38), separating amplitude (top) and phase (bottom).

for plotting (Figure 12). The rigid wall $z = \infty$ and the “capacitive” wall $z = 0.1i$, lead to the sharpest resonances and most abrupt phase jumps. The reactive wall $z = 0.1$ smooths the amplitude dips and phase jumps, with increased smoothing for positive capacity $z = 0.1(1 + i)$ and decreased smoothing for negative capacity $z = 0.1(1 - i)$.

Complex wavefields arise regardless of boundary conditions, if the parameter γ is complex (38), i.e., for complex wavenumber k in equation (35) or frequency ω . The odd wavefunction H has (39a) the same modulus or amplitude for complex conjugate values of γ , which takes the values

$$\gamma = 1 \pm 0.1i, \quad 1 \pm 0.2i, \quad (64)$$

for plotting (Figure 13); the amplitude (bottom) increases faster towards the free stream $\zeta < 0$ for larger $|\text{Im}(\gamma)|$, and all waveforms coalesce at the critical layer $\zeta = 0$, where the wavefield is zero $H(0) = 0$. The variation of the acoustic pressure towards the wall is small, and not too sensitive to γ . Concerning the phase (top), apart from a phase jump of π at the critical layer, it does not vary towards the wall. The phase varies more towards the free stream, and changes sign passing to the conjugate $\gamma \rightarrow \gamma^*$, because this corresponds to the conjugate waveform $H(\zeta) \rightarrow H^*(\zeta)$. The phase jumps (top) are more smoothed for positive capacity $\gamma = 1 + 0.1i, 1 + 0.2i$ than for negative capacity $\gamma = 1 - 0.1i, 1 - 0.2i$, but are not too sensitive to the magnitude of the capacity $|\text{Im}(\gamma)| = 0.1, 0.2$; conversely, the amplitude (bottom) is not too sensitive to positive $\text{Im}(\gamma) = \pm 0.1, \pm 0.2$ or negative capacity, but the amplitude is larger $|\text{Im}(\gamma)| = 0.2$ for larger capacity than

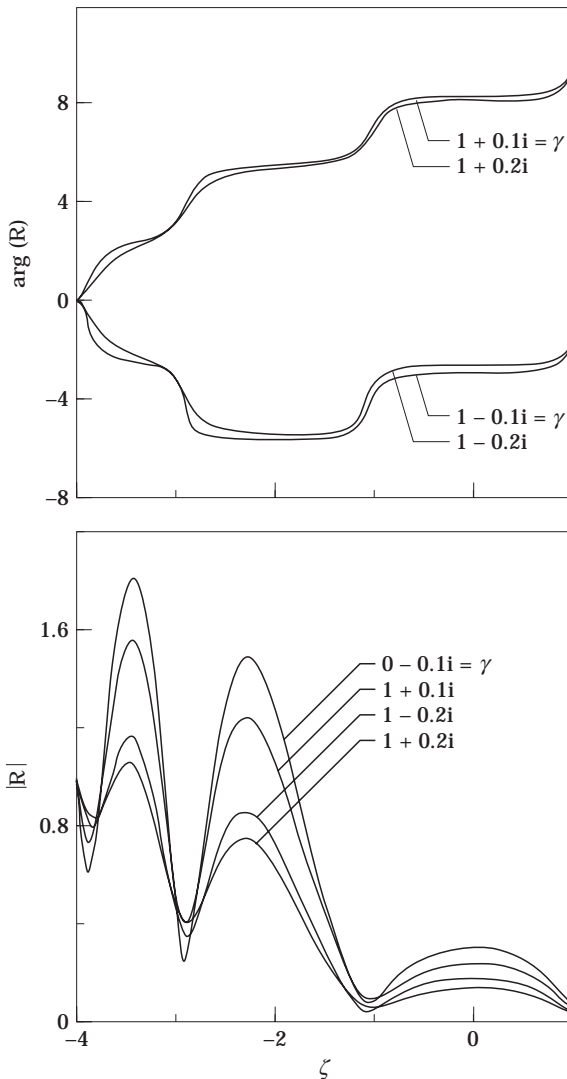


Figure 16. As for Figure 15 for a wall with specific impedance $z = 0.1$.

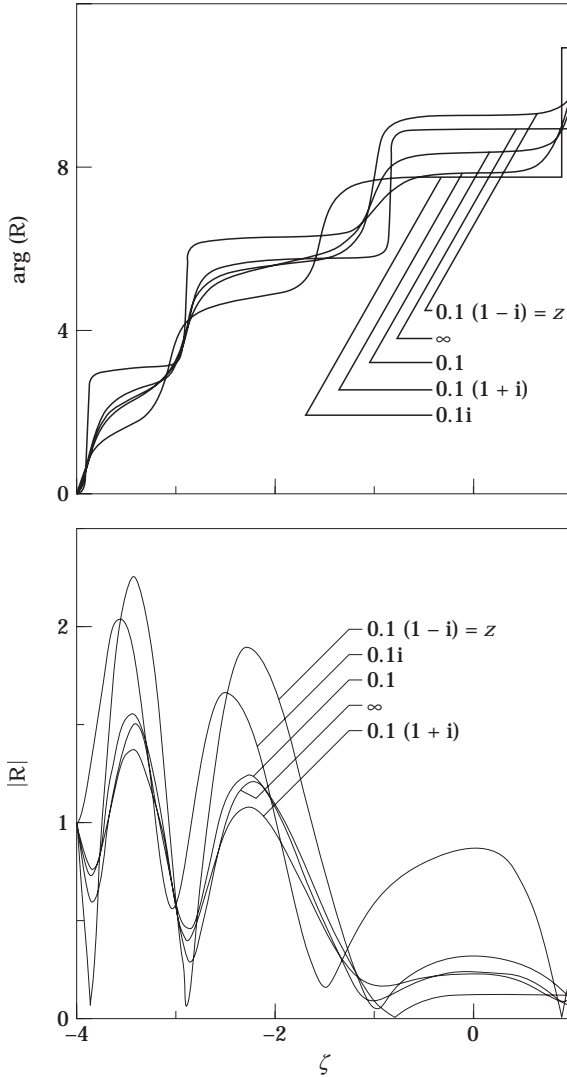


Figure 17. As for Figure 15, for several types of wall: rigid $z = \infty$, reactive $z = 0.1$, capacitive $z = 0.1i$, and impedance $z = 0.1(1 \pm i)$.

for smaller $|\text{Im}(\gamma)| = 0.1$, the difference between the two increasing away from the critical layer towards the free stream.

For the same values of the parameter γ in equation (64), the even wavefunction J in equation (40a), has similar amplitude and phase (Figure 14) towards the free stream $\zeta < 0$, i.e., the amplitude oscillates and is not sensitive to the sign of $\text{Im}(\gamma)$ whereas the phase changes sign with the sign of $\text{Im}(\gamma)$. The critical layer $\zeta = 0$ is a local amplitude maximum, with the acoustic pressure decaying towards the wall $\zeta > 0$. The phase changes are small near the critical layer.

The effect of complex values (64) of γ is also shown for the total acoustic field (42), with normalization (61a, b) to the value at $\zeta = -4$ and for a rigid wall at $\zeta = \alpha = (\omega/q)^2$. The amplitude (Figure 15, bottom) varies little between the critical

layer $\zeta = 0$ and the wall $\zeta > 0$, and the phase (Figure 15, top) is almost constant. Towards the free stream $\zeta < 0$, there is a phase jump of π where the amplitude vanishes, and larger amplitude oscillations for smaller $|\text{Im}(\gamma)|$. A change of sign of $\text{Im}(\gamma)$ does not change the amplitude, but reverses the phase.

The same normalization (61a, b) and parameters (64), replacing a rigid $z = \infty$ by an impedance $z = 0.1$ wall, leads to noticeable changes. The amplitude (Figure 16, bottom) has a local maximum at the critical layer $\zeta = 0$, decays towards the wall $\zeta > 0$ and oscillates towards the free stream $\zeta < 0$ as before; however, the amplitudes are distinct for different γ , increasing in the sequence $\gamma = 1 + 0.2i$, $1 - 0.2i$, $1 + 0.1i$, $1 - 0.1i$. The phase (Figure 16, top) reverses sign with $\text{Im}(\gamma)$ as before, but only for $\zeta < -2$, whereas for $\zeta > -2$ it evolves the same way regardless of the sign of $\text{Im}(\gamma)$.

The final set of plots retains the normalization (61a, b) of the acoustic pressure at $\zeta = -4$, fixes the parameter (38) at a complex value $\gamma = 1 + 0.1i$, and considers several wall impedances (63). The amplitude (Figure 17, bottom) has a local maximum at the critical layer $\zeta = 0$, and decays towards the wall $\zeta > 0$, with larger value at the maximum and more tendency to oscillate towards the wall for a capacitive wall $z = 0.1i$. Towards the free stream $\zeta < 0$ there are oscillations with amplitude increasing in the order $= 0.1(1 + i)$, ∞ , 0.1 , $0.1i$, $0.1(1 - i)$. The phase (Figure 17, top) shows jumps at the nodes of the waveform; the phase jumps of π are sharper for the capacitive wall $z = 0.1i$, and are slightly rounded off for the rigid wall and smoother for other values of the wall impedance.

5. DISCUSSION

As general remarks it is noted that (a) the critical layer for sound in a shear flow resembles the transition layers of atmospheric waves and other waves in fluids [28, 30, 31, 38, 65] in that the oscillations die out in its vicinity, and the waveforms separate, according to the parameters of the wave (frequency, wavenumber) and background medium (scales of variation of properties), only as one moves away from the critical layers, and (b) it is clear that there is absorption of sound when the critical layer is transversed, in the sense that the acoustic pressure tends to be smaller and oscillate less at the wall, than at some distance into stream. Thus the presence of an acoustic critical layer could explain the attenuation of sound observed to occur in boundary layers. For a range of boundary conditions, including rigid and compliant walls, it is observed that the acoustic pressure tends to be maximum at the critical layer, and to shift from compression to depression for higher vorticity, lower frequency or smaller wavenumber.

In retrospect, the problem of sound propagation in a linear shear flow has been reconsidered, leading to what is arguably the simplest solution in the literature: a decomposition into solutions which are symmetric and skew-symmetric relative to the critical layer. This solution follows by straightforward application of the Frobenius–Fuchs method to the acoustic wave equation, starting from the fundamental observation that there is only one singularity at finite distance, which is regular, and corresponds to the critical layer. The plotting of these solutions shows that the oscillations of the acoustic field, which occur towards the free

stream, beyond the critical layer, die out in its neighbourhood, and are replaced by a slow monotonic variation, in the region of the boundary layer, between the critical layer and the wall. This can be loosely interpreted as meaning that the critical layer acts as a reflector of sound waves coming from the free stream, leaving only an evanescent acoustic field between the critical layer and the wall. The present paper does not consider the question of non-linear evolution of the critical layer, because the present theory gives no singularity there, i.e., linear non-dissipative aeroacoustics [63, 64] is a self-consistent model.

A point discussed in the literature is the possible distinction between "acoustic" and "hydrodynamic" modes, as two types of perturbations of a shear flow, e.g., in the case of a sound source in a duct containing a shear flow [12] the "acoustic" modes were ascribed to the source and the "hydrodynamic" modes to the existence of a critical layer; this classification would appear to imply that, in the absence of an acoustic source, only "hydrodynamic" modes exist. In order to check this, it is necessary to have first a definition of what an "acoustic" or "hydrodynamic" mode is. It is usual to associate "acoustic" modes with two properties: (i) being irrotational; (ii) propagating at the sound speed. It has been shown [2] that small amplitude perturbations of a linear shear flow cannot satisfy (i) and (ii) simultaneously: i.e., (a) perturbations travelling at sound speed are rotational and (b) irrotational perturbations do not travel at sound speed. One could try to relax the definition of "acoustic" mode to just one condition, e.g., (i) of being irrotational, allowing a distinction from the "hydrodynamic" mode, which would be incompressible (or divergence-free). It will be shown in the Appendix that, for small amplitude perturbations of a linear shear flow, the vorticity and dilatation are in a constant ratio, and hence "acoustic" and "hydrodynamic" modes are always coupled, in the sense that a general perturbation is both rotational and compressive; an equivalent conclusion, is that a separation into "acoustic" and "hydrodynamic" modes is an arguable or dubious notion, for small amplitude perturbations of a linear shear flow.

ACKNOWLEDGMENT

The author is grateful to the referees for raising a number of issues left unaddressed in the first version of the manuscript.

REFERENCES

1. D. C. PRIDMORE-BROWN 1958 *Journal of Fluid Mechanics* **4**, 393–406. Sound propagation in a fluid flowing through an attenuating duct.
2. W. MOHRING, E. A. MULLER and F. OBERMEIER 1983 *Reviews of Modern Physics* **55**, 707–724. Problems in flow acoustics.
3. D. H. TACK and R. F. LAMBERT 1965 *Journal of the Acoustical Society of America* **38**, 655–666. Influence of shear flow on sound attenuation in lined ducts.
4. P. MUNGUR and H. E. PLUMBLEE 1969 *NASA SP-207*, 305–327. Propagation and attenuation of sound in a soft walled annular duct containing a sheared flow.
5. S. MARIANO 1971 *Journal of Sound and Vibration* **19**, 261–275. Effect of wall shear layers on the sound attenuation in acoustically lined rectangular ducts.

6. A. S. HERSH and I. CATTON 1971 *Journal of the Acoustical Society of America* **50**, 992–1003. Effects of shear flow on sound propagation in rectangular ducts.
7. W. EVERSMAN 1971 *Journal of the Acoustical Society of America* **39**, 1372–1380. Effect of boundary layer on the transmission and attenuation of sound in an acoustically treated circular duct.
8. W. EVERSMAN and R. J. BECKENMEYER 1972 *Journal of the Acoustical Society of America* **52**, 216–225. Transmission of sound in ducts with thin shear layers: convergence to the uniform flow case.
9. P. N. SHANKAR 1971 *Journal of Fluid Mechanics* **47**, 81–91. Acoustic refraction by duct shear layers.
10. P. N. SHANKAR 1972 *Journal of Sound and Vibration* **22**, 233–296. Acoustic refraction and attenuation in cylindrical and annular ducts.
11. S. H. KO 1972 *Journal of Sound and Vibration* **22**, 193–210. Sound attenuation in acoustically lined circular ducts in the presence of uniform flow and shear flow.
12. M. A. SWINBANKS 1975 *Journal of Sound and Vibration* **40**, 51–76. Sound field generated by a source distribution in a long duct carrying sheared flow.
13. T. F. BALSA 1976 *Journal of Fluid Mechanics* **74**, 193–208. The far-field of high-frequency convected, singularities in sheared flows, with application to jet noise prediction.
14. T. F. BALSA 1976 *Journal of Fluid Mechanics* **76**, 443–456. Refraction and shielding of sound from a source in a jet.
15. M. K. MYERS and S. L. CHUANG 1983 *American Institution of Aeronautics and Astronautics Journal* **22**, 1234–1241. Uniform asymptotic approximations for duct acoustic modes in a thin boundary-layer flow.
16. D. B. HANSON 1984 *Journal of Sound and Vibration* **92**, 591–598. Shielding of propfan cabin noise by the fuselage boundary layer.
17. M. ALMGREN 1986 *Journal of Sound and Vibration* **105**, 321–327. Acoustic boundary layer influence in scale model simulation of sound propagation: theory and numerical examples.
18. S. ISHII and T. KAKUTANI 1987 *Journal of Sound and Vibration* **113**, 127–139. Acoustic waves in parallel shear flows in a duct.
19. M. GOLDSTEIN and E. RICE 1973 *Journal of Sound and Vibration* **30**, 79–84. Effect of shear on duct wall impedance.
20. D. S. JONES 1977 *Philosophical Transactions of the Royal Society* **A284**, 287–328. The scattering of sound by a simple shear layer.
21. D. S. JONES 1978 *J. Inst. Math. Appl.* **21**, 197–209. Acoustics of a splitter plate.
22. J. N. SCOTT 1979 *American Institution of Aeronautics and Astronautics Journal* **17**, 237–245. Propagation of sound waves through a linear shear layer.
23. S. P. KOUTSOYANNIS 1980 *Journal of Sound and Vibration* **68**, 187–202. Characterization of acoustic disturbances in linearly sheared flows.
24. S. P. KOUTSOYANNIS, K. KARAMCHTI and D. C. GALANT 1980 *American Institution of Aeronautics and Astronautics Journal* **18**, 1446–1450. Acoustic resonances and sound scattering by a shear layer.
25. D. KÜCHEMAN 1938 *Zeits. angew. Math. Mech.* **30**, 79–84. Strömungsbewegungen in einer Gasströmung mit Grenzschicht.
26. E. W. GRAHAM and B. B. GRAHAM 1968 *Journal of the Acoustical Society of America* **46**, 169–175. Effect of a shear layers and plane waves of sound in a fluid.
27. J. R. BOOKER and F. P. BRETHERTON 1967 *Journal of Fluid Mechanics* **27**, 513–529. A critical layer for internal gravity waves in a shear flow.
28. J. S. TURNER 1973 *Bouyancy Effects in Fluids*. Cambridge: Cambridge University Press.
29. M. J. LIGHTHILL 1978 *Waves in Fluids*. Cambridge: Cambridge University Press.
30. H. P. GREENSPAN 1968 *Theory of Rotating Fluids*. Cambridge: Cambridge University Press.

31. P. G. DRAZIN and W. H. REID 1981 *Hydrodynamic Stability*. Cambridge: Cambridge University Press.
32. M. YANOWITZ 1967 *Canadian Journal of Physics* **45**, 2003–2008. Effect of viscosity on vertical oscillations of an isothermal atmosphere.
33. P. LYONS and M. YANOWITZ 1974 *Journal of Fluid Mechanics* **66**, 273–288. Vertical oscillations in a viscous and thermally conducting isothermal atmosphere.
34. L. M. B. C. CAMPOS 1983 *Wave Motion* **5**, 1–14. On three-dimensional acoustic-gravity waves in model non-isothermal atmospheres.
35. J. F. MCKENZIE 1973 *Journal of Fluid Mechanics* **58**, 709–723. On the existence of critical layers, with application to hydromagnetic waves.
36. L. M. B. C. CAMPOS 1983 *Journal of Physics* **A16**, 417–437. On magneto-acoustic-gravity waves propagating or standing vertically in an atmosphere.
37. L. M. B. C. CAMPOS 1988 *Journal of Physics* **A21**, 2911–2930. On oblique Alfvén waves in a viscous and resistive atmosphere.
38. L. M. B. C. CAMPOS 1989 *Geophys. Astrophys. Fluid Dyn.* **40**, 93–132. On the properties of hydromagnetic waves in the vicinity of critical levels and transition layers.
39. L. M. B. C. CAMPOS 1993 *Wave Motion* **17**, 101–112. Exact and approximate methods for hydromagnetic waves in dissipative atmospheres.
40. L. M. B. C. CAMPOS 1993 *European Journal of Mechanics* **B12**, 187–216. Comparison of exact solutions and phase mixing approximation for dissipative Alfvén waves.
41. L. M. B. C. CAMPOS and N. L. ISAEVA 1992 *Journal of Plasma Physics* **48**, 415–434. On vertical spinning Alfvén waves in a magnetic flux tube.
42. A. H. NAYFEH, J. E. KAISER and D. P. TELIONIS 1975 *American Institution of Aeronautics and Astronautics Journal* **13**, 130–153. Acoustics of aircraft engine-duct systems.
43. L. M. B. C. CAMPOS 1986 *Review of Modern Physics* **58**, 117–182. On waves in gases. Part I: acoustics of jets, turbulence and ducts.
44. L. M. B. C. CAMPOS 1986 *Journal of Sound and Vibration* **110**, 41–57. On linear and non-linear wave equations for the acoustics of high-speed potential flows.
45. H. S. TSIEN 1952 *Journal of the American Rocket Society* **22**, 139–150. The transfer functions of rocket nozzles.
46. A. POWELL 1960 *Journal of the Acoustical Society of America* **32**, 1640–1646. Theory of sound propagation through ducts carrying high-speed mean flows.
47. N. A. EISENBERG and T. W. KAO 1971 *Journal of the Acoustical Society of America* **49**, 169–175. Propagation of sound in a variable area duct with a steady, compressible mean flow.
48. L. M. B. C. CAMPOS 1984 *Zeitschrift für Flugwissenschaften und Weltraumforschung* **8**, 97–109. On the propagation of sound in nozzles of varying cross-section containing a low Mach number mean flow.
49. L. M. B. C. CAMPOS 1987a *Journal of Sound and Vibration* **117**, 131–151. On longitudinal propagation in convergent and divergent nozzle flows.
50. L. M. B. C. CAMPOS and F. J. P. LAU 1996 *Journal of the Acoustical Society of America* **100**, 355–363. On sound in an inverse sinusoidal nozzle with low Mach number mean flow.
51. L. M. B. C. CAMPOS and F. J. P. LAU 1996 *Journal of Sound and Vibration* **196**, 611–633. On the acoustics of low Mach number bulged, throated and baffled nozzles.
52. R. MANI 1980 *Philosophical Transactions of the Royal Society* **A371**, 393–412. Sound propagation in parallel sheared flows in ducts: the mode estimation problem.
53. D. I. BLOKHINTSEV 1946 *Journal of the Acoustical Society of America* **18**, 322–346. The propagation of sound in and moving medium.
54. L. M. B. C. CAMPOS 1978 *Journal of Fluid Mechanics* **89**, 723–749. On the spectral broadening of sound by turbulent shear layers. Part I: scattering by interfaces and refraction in turbulence.

55. L. M. B. C. CAMPOS 1978 *Journal of Fluid Mechanics* **89**, 751–779. On the spectral broadening of sound by turbulent shear layers. Part II: broadening of experimental and aircraft noise.
56. S. M. CANDEL 1975 *Journal of Sound and Vibration* **41**, 207–232. Acoustic conservation principles and an application to plane and modal propagation in nozzles and diffusers.
57. L. M. B. C. CAMPOS 1988 *Wave Motion* **10**, 193–207. On the generalizations of Doppler factor, local frequency, wave invariant and group velocity.
58. J. A. ADAM 1977 *Phys. Resp.* **86**, 217–316. Asymptotic solutions and spectral theory of linear wave equations.
59. A. R. FORSYTH 1902–6 *Theory of Differential Equations*. Cambridge: Cambridge University Press, six volumes.
60. A. R. FORSYTH 1927 *Treatise of Differential Equations*. London: MacMillan, sixth edition, 1926.
61. E. L. INCE 1954 *Differential Equations*. New York: Dover; 1926 edition.
62. E. G. C. POOLE 1935 *Linear Differential Equations*. New York: Dover.
63. M. E. GOLDSTEIN 1976 *Aeroacoustics*. New York: McGraw Hill.
64. A. D. PIERCE 1981 *Acoustics*. New York: McGraw-Hill.
65. L. M. B. C. CAMPOS 1987 *Reviews of Modern Physics* **59**, 363–462. On waves in gases. Part II: interaction of sound with magnetic and internal modes.
66. L. M. B. C. CAMPOS 1990 *Geophys. Astrophys. Fluid Dyn.* **48**, 193–215. On the dissipation of Alfvén waves in uniform and non-uniform magnetic fields.
67. E. T. WHITTAKER and G. N. WATSON 1927 *Course of Modern Analysis*. Cambridge: Cambridge University Press.
68. P. M. MORSE and H. FESHBACH 1953 *Methods of Theoretical Physics*. New York: McGraw-Hill; two volumes.
69. L. M. B. C. CAMPOS 1985 *Geophys. Astrophys. Fluid Dyn.* **32**, 217–272. On vertical hydromagnetic waves in a compressible atmosphere under an oblique magnetic field.

APPENDIX: COUPLING OF DILATATION AND VORTICITY FOR SMALL AMPLITUDE PERTURBATIONS OF A LINEAR SHEAR FLOW

The remark that acoustic waves in a shear flow can have a critical layer or turning point has been made in the literature, e.g., [2, 12, 13], as well as the discussion of “hydrodynamic” and “acoustic” modes [12, 2]. The approach to the problem in the latter reference [2] will be further developed in this appendix. The starting point is the conservation of vorticity $\vec{\Omega}$ in an isentropic flow, as stated by Kelvin’s circulation theorem

$$\vec{\Omega} \equiv \nabla \wedge \vec{v}; \quad \partial \vec{\Omega} / \partial t = \nabla \wedge (\vec{v} \wedge \vec{\Omega}). \quad (65)$$

The conservation law for an axial vector, like the vorticity $\vec{\Omega}$, is distinct from the conservation law for a scalar density, like the mass density ρ :

$$\partial \rho / \partial t + \nabla \cdot (\rho \vec{v}) = 0. \quad (66)$$

The closest form of the two equations is

$$D \vec{\Omega} / dt = (\vec{\Omega} \cdot \nabla) \vec{v} - \vec{\Omega} (\nabla \cdot \vec{v}), \quad D \rho / dt = -\rho (\nabla \cdot \vec{v}), \quad (67a, b)$$

where

$$D/dt \equiv \partial/\partial t + \vec{V} \cdot \nabla \quad (68)$$

is the material derivative. From equations (67a, b) follows readily the Beltrami equation

$$D(\vec{\Omega}/\rho)/dt = \rho^{-1}(\vec{\Omega} \cdot \nabla)\hat{v}, \tag{69}$$

which is a possible basis for attempting to distinguish between ‘‘acoustic’’ and ‘‘hydrodynamic’’ modes [2].

In the present case, of plane perturbation (v_x, v_y) of a unidirectional linear shear ($qy, 0$), the vorticity lies in the orthogonal plane,

$$\vec{\Omega} = (q + \bar{\Omega}) \hat{e}_z, \quad \bar{\Omega} \equiv \partial v_y/\partial x - \partial v_x/\partial y, \tag{70a, b}$$

and its perturbation (70b) involves the y -component of the velocity perturbation spectrum (45), and the derivative with regard to y of the x -component:

$$v_x(x, y, t) = \iint_{-\infty}^{\infty} V_x(y; k, \omega) e^{i(kx - \omega t)} dk d\omega. \tag{71}$$

Thus Beltrami equation reduces to

$$0 = D(\Omega_z/\rho)/dt, \tag{72}$$

which may be linearized as

$$D[(\bar{\Omega}\rho_0 - \bar{\rho}q)/\rho_0^2]/dt = 0, \tag{73}$$

where $\bar{\rho}$ is the density perturbation.

The latter satisfies the linearized equation (66) of continuity:

$$\partial \bar{\rho}/\partial t + U \partial \bar{\rho}/\partial x + \rho_0(\nabla \cdot \hat{v}) = 0, \tag{74}$$

Upon introducing the spectrum of the mass density

$$\bar{\rho}(x, y, t) = \iint_{-\infty}^{+\infty} E(y; k, \omega) e^{i(kx - \omega t)} dk d\omega, \tag{75}$$

the equation of continuity becomes

$$\rho_0 \tilde{A} = i(\omega - kU)E = i\omega_* E, \tag{76a}$$

where ω_* is the Doppler shifted frequency (7), and \tilde{A} is the spectrum of the dilatation,

$$A \equiv \partial v_x/\partial x + \partial v_y/\partial y. \tag{76b}$$

The spectra of the vorticity (70b) and dilatation (76b),

$$\tilde{\Omega} = ikV_y - V'_x, \quad \tilde{A} = ikV_x + V'_y, \tag{77a, b}$$

following from equations (45) and (71), where the prime denotes the derivative with regard to y .

Upon bearing in mind the linearization of the material derivative (68) in spectral form,

$$D/Dt = \partial/\partial t + U\partial/\partial x = -i(\omega - kU) = -i\omega_*, \quad (78)$$

the spectral form of the Beltrami equation (73) is

$$0 = -i(\omega_*/\rho_0^2)(\tilde{\Omega}\rho_0 - Eq). \quad (79)$$

Substituting equation (76a) into this yields

$$0 = -i(\omega_*/\rho_0)(\tilde{\Omega} - q\tilde{A}/i\omega_*). \quad (81)$$

The conclusion is

$$\tilde{\Omega}/\tilde{A} = -iq/\omega_* \equiv -iq/(\omega - kqy). \quad (82)$$

Thus the spectra of the vorticity and dilatation are out-of-phase by $\pi/2$, and their ratio equals the ratio of the vorticity of the mean flow (constant for a linear shear) to the Doppler shifted frequency. It is thus clear that perturbations of vorticity and dilatation are coupled, for small amplitude perturbations of a linear shear flow. The only exception is the critical layer, where the Doppler shifted frequency vanishes, and hence the dilatation also vanishes, by (76a).